

Detection of polycyclic aromatic hydrocarbon (PAH) compounds in artificial sea-water using surface-enhanced Raman scattering (SERS)

Olivier Péron^a, Emmanuel Rinnert^{a, *}, Michel Lehaitre^a, Philippe Crassous^b and Chantal Compère^a

^a IFREMER, Service Interfaces et Capteurs, BP 70, 29280 Plouzané, France

^b IFREMER, Laboratoire Environnement Profond, BP 70, 29280 Plouzané, France

*: Corresponding author : Emmanuel Rinnert, Tel.: +33 2 98 22 41 61; fax: +33 2 98 22 45 35, email address : Emmanuel.Rinnert@ifremer.fr

Abstract:

This paper reports an accurate synthesis of surface-enhanced Raman scattering (SERS) active substrates, based on gold colloidal monolayer, suitable for *in situ* environmental analysis. Quartz substrates were functionalized by silanization with (3-mercaptopropyl)trimethoxysilane (MPMS) or (3-aminopropyl)trimethoxysilane (APTMS) and they subsequently reacted with colloidal suspension of gold metal nanoparticles: respectively, the functional groups SH and NH₂ bound gold nanoparticles. Gold nanoparticles were prepared by the chemical reduction of HAuCl₄ using sodium tricitrate and immobilized onto silanized quartz substrates. Active substrate surface morphology was characterized with scanning electron microscopy (SEM) measurements and gold nanoparticles presented a diameter in the range 40–100 nm. Colloidal hydrophobic films, allowing nonpolar molecule pre-concentration, were obtained. The surfaces exhibit strong enhancement of Raman scattering from molecules adsorbed on the films. Spectra were recorded for two PAHs, naphthalene and pyrene, in artificial sea-water (ASW) with limits of detection (LODs) of 10 ppb for both on MPMS silanized substrates.

Keywords: Gold nanoparticles; Silanization; SERS; PAH detection; Sea-water; Sensor

1. Introduction

Since the discovery by Fleischmann et al. in 1974 [1] of an abnormally intense enhancement of the Raman signal of pyridine molecules adsorbed on the roughened surfaces of silver electrodes, the scientific community has shown an ever increasing interest in the surface-enhanced Raman scattering (SERS) effect. SERS is a very sensitive technique which has been extensively employed in the study of a wide range of molecules and using different types of surfaces like colloidal metal nanoparticles, roughened metal foils, island crystal films... In SERS measurements, huge Raman enhancements, up to 106-fold [2], [3] and [4] the normal Raman signal of non-adsorbed molecules, have been observed when molecules are adsorbed on active metallic surfaces (Au, Ag, Cu...) which exhibit high optical reflectivity. More recently, enhancement factors of up to 1014 to 1020 were obtained in single-molecule detection experiments [5] S. Nie and S.R. Emory, *Science* 275 (1997), p. 1102. Full Text via CrossRef | View Record in Scopus | Cited By in Scopus (2164)[5], [6], [7] and [8]. Two theories help to explain the Raman enhancement origin: the short-range chemical model and the long-range electromagnetic model [9], [10] and [11]. The first one is related to a charge transfer between the roughened surface and the target molecule via an increase in adsorbed molecule polarisability. The second one is linked to the excitation of

surface plasmons (free electrons oscillations) leading to an increase in the local electromagnetic field. A final Raman enhancement of an adsorbed molecule can be considered as the coupling of both mechanisms. However, the electromagnetic one is known to contribute predominantly to the Raman enhancement compared to chemical one which is much smaller (10^2) [12].

SERS can be considered as an alternative to the inherent low cross-section of normal Raman scattering. In the investigation of chemical pollutions, such as PAH low concentration (ppm) or trace concentration (ppb) in sea-water, SERS effect reveals an immense potential regarding the marine environment. In this study, SERS-active substrates able to act as pre-concentrate hydrophobic compounds were developed. The strategy for obtaining SERS-sensitive substrates was to graft silanes with terminal function groups, such as -SH or -NH₂, having an affinity for metal particles. Gold is bound to the surface through covalent interactions if the functional group is a thiol or an amine [13-15]. Although silver presents a higher SERS response with an enhancement factor 10-100 fold greater than gold, Au was chosen here on account of AgCl formation on silver surfaces in the marine medium [16]. The silanes are bound chemically to the substrate via hydroxyl groups which are already present at the SiO₂ surface [17]. With (3-mercaptopropyl)trimethoxysilane (MPMS) and (3-aminopropyl)trimethoxysilane (APTMS) silanizations, the quartz surface properties are modified and the nonpolar -CH₂ groups give hydrophobic surfaces. Consequently nonpolar molecules, such as PAHs, are preferentially adsorbed on the substrate surface. Previous studies have already been undertaken works were on PAH detection based on sol-gel process with Au or Ag particles embedded in a methyl/ethyl-tetraethoxysilane (MTEOS/ETEOS) precursor [18,19] through the EU funded MISPEC project. In Lutch *et al.* [19], LODs of 430 ppb naphthalene concentration were notified with a 785 nm Raman excitation. More recently within the scope of screening development, a solution of five PAHs in sea-water with LODs

of 37.5 μM and 0.1 μM for naphthalene and pyrene respectively, was analyzed by Schmidt *et al.* [20]. Besides, published literature has reported the influence of adsorption and complexation with PAHs on host calixarenes (nonpolar cavities) [21,22].

There are further studies on such functionalization for which SERS measurements were recorded. For example, APTMS silanization was used to detect bi-ethylene-pyridine [23] and tetrakis(methyl-pyridyl)porphyrin [24]. As for MPMS, mercaptoundecanol SERS spectra were recorded [25], benzenethiol as a molecular probe was detected in Jung *et al.* [26] and Rhodamine 6G detection was carried out [27]. Moreover, ppm levels of PAHs were detected thanks to the alkyl chain of propanethiol by Costa *et al.* [28]; MPMS was used as a link to build self-assembly monolayers (SAMs). Furthermore, MPMS plays a role in various application fields: chelating ligands for use in the removal of heavy metal ions in solution [29], electroless plating of silver on SAMs [30], free DNA biosensors characterized with electrochemical impedance spectroscopy [31] or silanized-protection versus steel corrosion [32].

This article demonstrates the interest of developing sensitive sensors for sea-water analyses with the aim of detecting PAHs. As far as we know, this paper relates for the first time PAHs pre-concentration onto APTMS or MPMS.

2. Experimental

2.1. Instrumentation

SERS spectra of naphthalene and pyrene solutions were recorded at room temperature with a Raman spectrometer (Labram HR800-Jobin Yvon) using the 632.8 nm excitation line

of a He-Ne laser (power ~ 0.1 mW at the sample) in retrodiffusion geometry. The laser beam was focused through a water immersion lens (x100, NA = 1) to a spot of around $1 \mu\text{m}^2$. Scattered radiation was collected at 180° relative to the excitation beam and detected with an Andor CCD cooled by the Peltier effect. A 300 g/mm grating coupled to a 800 mm spectrograph allows a spectral resolution of around 2 cm^{-1} . Spectral calibration was performed on silicium samples (at 520 cm^{-1}). Two stage edge filters allow Raman Stokes studies. The accumulation times were 1 s, 10 s or 20 s.

A visible JenWay-6400 spectrometer was used to record the extinction spectra of colloidal solutions in the spectral region between 400 and 900 nm (resolution 0.2 nm). Analyzed solutions were diluted in distilled water (25% v v⁻¹). Water spectrum was used as the baseline. A tungsten light was employed as the exciting source.

Concerning colloidal film extinction spectra, a Raman spectrometer, without any edge filter, was used with a white exciting light through a lens (x50, NA = 0.75). In order to record the spectrum baseline, the bare substrate was illuminated.

Scanning electron microscopy (SEM) measurements were done with a field emission scanning electron microscope (FEI-Quanta200). Before loading into the observation chamber, the samples were coated with a thin Au film (~ 10 -15 nm) by sputtering to avoid a surface charging effect.

2.2. Chemicals and materials

$\text{HAuCl}_4 \cdot 3\text{H}_2\text{O}$ and (3-aminopropyl)trimethoxysilane (APTMS, 95%) were purchased from Acros Organics. Hydrochloric acid (37%) and (3-mercaptopropyl)trimethoxysilane (MPMS, 95%) were obtained from Sigma-Aldrich. Sodium tricitrate was purchased from

Prolabo, nitric acid (65%) was from Merck, hydrogen peroxide (30%) was from J.T. Baker, ammonium hydroxide (33%) was from Riedel-de-Haën, methanol and ethanol were of analytical grade from Fisher. Naphthalene from Fisher and pyrene from Cerilliant were used as analytical molecular references.

The quartz substrates were tailored with 8 mm diameter and 0.8 mm thickness from Heraeus. Quartz were cleaned using aqua regia (25% HCl, 25% HNO₃, 50% distilled water v v⁻¹) and afterwards a base “piranha” solution (75% NH₄OH, 25% H₂O₂ v v⁻¹) to eliminate organic compounds and to promote hydroxylated surfaces.

2.3. Colloidal suspension of gold nanoparticles and PAH solutions

Colloidal suspensions of gold nanoparticles were prepared according to the method described by Frens [33]. Such a metal preparation technique has been used in different studies [15,23,34,35] and consists in the reduction of HAuCl₄ or AgNO₃ by sodium tricitrate. After the addition of a reducing agent, the gold particles start to form during a process known as nucleation and subsequently grow. Here, 10 mL of sodium tricitrate at 8.10⁻³ M was slowly added to 10 mL of boiling tetrachloroauric acid at 2.10⁻³ M while stirring. The reactor was placed on a hot plate and magnetically stirred. The mixture of both solutions was refluxed for one hour. Temperature mixture was controlled with a thermometer (~ 90 °C). The initially dark-grey solution turned to a red-violet hue following two to three minutes of continued boiling. After one hour boiling, the mixture was cooled at room temperature under stirring.

The naphthalene solution was prepared by dissolving PAH in methanol wherein it is more soluble and diluted in distilled water. Naphthalene in pure water at 25 °C is soluble at 31.8 mg.L⁻¹. A 25 ppm naphthalene solution was prepared from 390 µL of 0.05 mol.L⁻¹

naphthalene methanol solution and the corresponding blank composed by 390 μL of methanol completed by 100 mL of pure water.

PAH solutions in artificial sea-water (ASW) were also obtained. A 10 ppm naphthalene solution and a 0.10 ppm pyrene solution both diluted to 10 ppb were achieved. Pyrene in pure water at 25 °C is soluble at 0.13 $\text{mg}\cdot\text{L}^{-1}$. The 10 ppm pyrene solution was prepared from 5 μL of 0.005 $\text{mol}\cdot\text{L}^{-1}$ pyrene methanol solution and the corresponding blank composed by 5 μL of methanol completed by 50 mL of ASW. ASW was prepared according to the ASTM D1141-90 norm [36].

2.4. Silanization - SERS substrates

Clean disk quartz substrates were vertically immersed in a 5% ($\text{v}\ \text{v}^{-1}$) methanol solution of MPMS or APTMS for four hours according to the results obtained by Seitz *et al.* [23]. After silanization, the substrates were rinsed several times in methanol, sonicated in methanol for twenty minutes to remove silane excess and dried for one hour at 100 °C in an air oven. Then, the silanized quartz were vertically dipped for one hour into the colloidal suspension of gold nanoparticles for the purpose of preparing Au nanoparticle films. In order to reach the most favorable conception recipe, some substrates were kept two days in the air before immersion in the colloidal solution. Finally, SERS-active substrates were dried for ten minutes at 100 °C. Suitable substrates for adsorbed hydrophobic molecule species and SERS measurements were thus synthesized. Scheme 1 presents a schematic representation of the SERS substrate fabrication procedure.

Scheme 1 around here

3. Results and Discussion

3.1. Plasmon band (evolution)

After the silanized substrates were dipped in colloidal suspension, the extinction spectra were recorded in order to check the potential SERS activity (Fig. 1 A)). On the one hand, the samples which Au nanoparticles were deposited immediately after APTMS and MPMS silanization (case i)) show extinction spectra with a plasmon band centered around 540-548 nm. On the other hand, the extinction spectrum of the samples which Au nanoparticles were immobilized two days after MPMS silanization (case ii)) reveals a red shift around 554-557 nm of the plasmon band and a broad plasmon band (600-700 nm). Such a broad plasmon band has already been observed by Hajdukova *et al.* [24] in the course of different preparation procedures. The colloidal solution used for the SERS substrate fabrication presents a plasmon band centered around 530 nm. We noted that such a colloidal suspension leads to samples with extinction spectra centered around 540-548 nm or 554-557 nm. These results seem to indicate that particle self organization and the interaction between themselves are slightly modified. Figs. 1 B) and C) respectively show SEM images of APTMS and MPMS samples obtained following an immersion in colloidal suspension in case i). As expected, no significant difference appears between APTMS and MPMS functionalization. Fig. 1 D) presents the SEM image of a MPMS sample kept in the air for two days before immersion (case ii)). The latter shows a dense nanoparticle distribution with a couple of nanoparticles of large diameters. Size particles are in the range of 40-100 nm. When

comparing both MPMS extinction spectra, such results are in agreement with the shoulder of up 700 nm.

Figs. 1 around here

3.2. Spectroscopic characterization

A neat MPMS (95%) Raman spectrum and a MPMS active substrate SERS spectrum were collected (Fig. 2). The laser beam was focused through a conventional lens regarding SERS-active substrate and neat MPMS in order to avoid the silanization of the water immersion lens for the latter one. The neat MPMS (95%) Raman spectrum presents a S-H stretching mode of around 2580 cm^{-1} while in the SERS spectrum of active substrate, S-H vibration is not observed around the Au particles. This result is due to a thiol interaction process with Au particles. Such phenomena have already been observed and correspond to the S-H bond cleavages with the formation of a S-Au bond [37,38]. Consequently during the silanized substrate immersion stage into the colloidal suspension of gold nanoparticles, most of the S-H bond was cleaved and Au nanoparticles adhered to the substrate surface by a S-Au bond.

Besides, the spectral region from 2750 to 3100 cm^{-1} gives information about ν_{C-H} vibrations regarding the methyl and methylene groups. The spectra do not have the same features. In the spectrum of neat MPMS, the intensity of the symmetric $\nu_s(\text{CH}_3)$ vibrations at 2845 and 2945 cm^{-1} are substantial. In contrast concerning the spectrum of the MPMS SERS substrate, these modes assigned to the methoxy groups disappear and only $\nu(\text{C-H})$ associated to the methylene groups of the propyl chain exist. The Raman shifts and the assignments are

summarized in Table 1. The hydrolysis and the condensation of self-assembled monolayer films of MPMS on Au surfaces could explain Raman spectrum evolution [39]. In our case, hydrolysis and condensation occur during the silanization process (see Scheme 1).

Fig. 2 and Table 1 around here

3.3. Hydrophobic surface behavior – SERS activity

In order to evaluate the detection reversibility of sensors and optimal organosilane functionalization, tests were conducted on APTMS and MPMS SERS-active substrates. SERS spectra were recorded after naphthalene molecules were adsorbed onto the surface by depositing a drop of solution. The SERS substrates were then immersed for ten minutes in 10 mL of distilled water and SERS blank measurements were made. In the case of MPMS silanization, another rinsing in 10 mL of ethanol for ten minutes is required to eliminate totally the hydrophobic molecules. Results are presented in Figs. 3 A) and B). Hydrophobic molecule pre-concentrations on nonpolar surfaces result in a physisorption process. Physical adsorption is a type of adsorption in whereby the adsorbate is weakly linked to the surface only through Van der Waals interactions. More precisely here, London dispersion forces arise between nonpolar molecules. Concerning APTMS silanization, the functional amine group, with the free doublet, confers a sizeable polarity to the substrate surface. According to such results, we suggest that APTMS substrates allow reversible detection after water cleaning, whereas ethanol cleaning is necessary on MPMS substrates. MPMS substrates may be more sensitive towards hydrophobic molecule pre-concentrations due to stronger hydrophobic interactions.

Figs. 3 A) and B) around here

With a view to obtaining a complete study, naphthalene detection was acquired with different integration times of SERS spectra from different spots on the substrate surface (Fig. 4): 20 s and 1 s respectively for APTMS and MPMS silanization. The response of MPMS SERS-active substrate is much higher than that of APTMS. With respect to previous hypotheses, the high MPMS substrate predisposition in detecting and preconcentrating hydrophobic molecules was demonstrated. Even though Hajdukova *et al.* [24] underline the better efficiency of APTMS in binding Au nanoparticles, they detected adsorbed tetrakis(1-methyl-4-pyridyl)porphyrin (TMPyP) which are hydrophilic molecules. In our case, MPMS allows at the same time: quartz substrate silanization, Au nanoparticle binding and pre-concentration of hydrophobic molecules. As regards PAH detection in ASW, MPMS silanization is more relevant than that of APTMS.

Fig. 4 around here

3.4. PAH detection

Here, SERS substrate sensitivity was investigated by SERS measurements in artificial sea-water (ASW) of naphthalene and pyrene solutions. The experiments were conducted on MPMS silanized substrates kept in the air for two days during their preparation before being

immersed in colloidal suspension (case ii)). These SERS-active substrates present: extinction spectra with a broad plasmon band (600-700 nm) and a suitable pre-concentration of hydrophobic molecules for this study. With a 632.8 nm excitation line, such SERS substrates match the required conditions for detecting hydrophobic molecule traces. SERS spectra were recorded at different PAH concentrations. Between each concentration test, the samples were rinsed with ethanol and blank measurements were achieved in order to confirm sensor reversibility. The spectra were recorded from different spots on the substrate surface to promote SERS response homogeneity.

Thanks to the SERS spectra (Figs. 5 A) and B)), four points must be emphasized here: i) both PAHs, naphthalene and pyrene dissolved in ASW solution, exhibit a random intensity variation of the main characteristic Raman peaks, ii) under excitation the organic part of the active substrate seems to continually evolve, iii) adsorbed PAHs onto gold surface can be damaged and iv) LODs of these PAHs in ASW.

Fig. 5 A) and B) around here

Concerning the first point a well known theory [40], which stipulates that the vibrational parallel modes to the plane of the surface are the least enhanced modes, could explain the peak intensity variations. According to the surface selection rule and the adsorbate vibrational mode, different orientations and tilts of PAH molecules on substrate surface could occur [41]. Moreover, Nie & Emory [5] have shown that the SERS signal also depends on how nanoparticles are oriented with respect to the light polarization axis.

Concerning the evolution of the organic part under laser excitation, the origin remains uncertain but during the reduction process of gold nanoparticles, sodium tricitrate excess and oxidation products still remain in the colloids. The displacement of these species arising from competitive adsorption on the metal surface could be responsible for changes in the spectra features [42].

In addition, chemical oxidation phenomena of PAHs could occur in the case of PAH adsorption on gold island films [28]. Here, SERS substrate surfaces present a different catalytic activity as regards chemical species with free spaces on their surfaces. Moreover in our case, the intensity of the extinction spectra and of the laser power are lower.

As shown in Figs. 5 A) and B), LODs of 10 ppb for both PAHs, naphthalene and pyrene in ASW, were performed. Concerning naphthalene trace detection, the main peaks centered on 760 and 1380 cm^{-1} are preferentially considered. In the pyrene case, peaks centered on 590 and 1406 cm^{-1} with a higher intensity were preferentially studied. The peaks at 1575 cm^{-1} for naphthalene, 1594 and 1630 cm^{-1} for pyrene can not be easily analyzed since the organic part, *i.e.* MPMS and sodium tricitrate excess, presents Raman signals in this spectral region. Such results confirm SERS MPMS substrate performance in relation to hydrophobic sensitivity and sensors. We can not draw any conclusions on the evolution of the spectral intensity of the Raman peaks versus PAH concentration in so far as isolated sites on the surface, called hot spots, give rise to intense local plasmon fields. Moreover, 10 ppb LODs in ASW for both PAHs with an integration time of 10 s could lead to a more sensitive detection by increasing the integration time of the experiment. In this way a sub-ppb detection sensor may be obtained with a reasonable resolution of signal/noise > 10 on the main characteristic Raman peaks.

4. Conclusions

This present study has demonstrated that Au-colloidal hydrophobic films synthesized by quartz silanization provide, PAH pre-concentration and as well as a SERS effect. Surfaces exhibit a strong enhancement of Raman scattering from nonpolar molecules adsorbed on the films and PAH detection in artificial sea-water (ASW) was performed. A LOD of 10 ppb was found for naphthalene and pyrene ASW solutions. Such results were obtained with MPMS surfaces which exhibit a broad plasmon band and a red shift. These MPMS SERS-active substrates are very interesting for future *in situ* applications. The geometry and the chemical stability of the substrates match with our home-made *in situ* Raman spectrometer [20].

Acknowledgements

This project was supported by ANR financing (P2IC: Discomar) and carried out in conjunction with the Laboratoire de Nanotechnologie et d'Instrumentation Optique (LNIO) - Université de Technologie de Troyes (UTT).

Captions

Scheme 1 Schematic representation of the SERS substrate fabrication procedure. A) silanization step and B) after immersion in gold colloidal suspension.

Fig. 1 A) Extinction spectra of Au-colloidal films deposited immediately (case i)) after (a) APTMS silanization, (b) MPMS silanization and deposited two days later (case ii)) after (c) MPMS silanization. All spectra were smoothed by adjacent averaging (250 points).

SEM images (x100 000) of Au-colloidal films deposited immediately (case i)) after B) APTMS silanization, C) MPMS silanization and D) two days later (case ii)) after MPMS silanization.

Fig. 2 Neat MPMS (95%) Raman spectrum and MPMS active substrate SERS spectrum. Integration time of 10 s.

Figs. 3 A) SERS spectra of naphthalene solution (25 ppm) adsorbed on APTMS surface, after water cleaning and blank. For comparison Raman spectrum of solid-state naphthalene is also given. B) SERS spectra of naphthalene solution (25 ppm) adsorbed on MPMS surface, after water and ethanol cleaning and blank. For comparison Raman spectrum of solid-state naphthalene is also given. Integration time of 10 s. * Naphthalene detection.

Fig. 4 SERS spectra of naphthalene solution (25 ppm) adsorbed on APTMS and MPMS surfaces with respectively 20 s and 1 s as integration times. For comparison Raman spectrum of solid-state naphthalene is also given.

Fig. 6 A) SERS spectra of artificial sea-water naphthalene solutions from 0 to 10 ppm, blank and for comparison Raman spectrum of solid-state naphthalene is also given. B) SERS spectra of artificial sea-water pyrene solutions from 0 to 0.1 ppm, blank and for comparison Raman spectrum of solid-state pyrene is also given. Integration time of 10 s.

Table1 Raman shifts and assignments in the spectral region from 2750 to 3100 cm^{-1} for neat MPMS and MPMS SERS substrate.

References

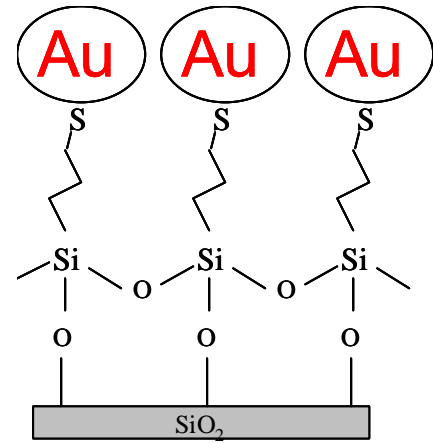
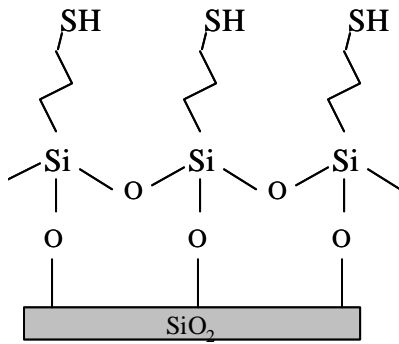
- [1] M. Fleischmann, P.J. Hendra, A.J. McQuillan, *Chem. Phys. Lett.* 26 (1974) 163.
- [2] M. Fleischmann, P.J. Hendra, A.J. McQuillan, R.L. Paul, E.S. Reide, *J. Raman Spectrosc.* 4 (1976), 269.
- [3] D.J. Jeanmaire, R.P. Van Duyne, *J. Electronanal. Chem.* 84 (1977) 1.
- [4] M.G. Albrecht, J.A. Creighton, *J. Am. Chem. Soc.* 99 (1977) 5215.
- [5] S. Nie, S.R. Emory, *Science* 275 (1997) 1102.
- [6] K. Kneipp, Y. Wang, H. Kneipp, L.T. Perelman, I. Itzkan, R.R. Dasari, M.S. Feld, *Phys. Rev. Lett.* 78 (1997) 1667.
- [7] K. Kneipp, H. Kneipp, G. Deinum, I. Itzkan, R.R. Dasari, M.S. Feld, *Appl. Spectrosc.* 52 (1998) 175.
- [8] K. Kneipp, H. Kneipp I. Itzkan, R.R. Dasari, M.S. Feld, *Chem. Phys.* 247 (1999) 155.
- [9] M. Moskovits, *Rev. Mod. Phys.* 57 (1985) 783.
- [10] A. Otto, *J. Raman Spectrosc.* 22 (1991) 743.
- [11] A. Otto, I. Mrozek, H. Grabhorn, W. Akemann, *J. Phys. Condens. Matter.* 4 (1992) 1143.
- [12] J.E. Ivanecky III, C.M. Child, Alan Campion, *Surf. Sci.* 325 (1995) 428.
- [13] R.G. Nuzzo, B.R. Zegarski, L.H. Dubois, *J. Am. Chem. Soc.* 109 (1987) 733.
- [14] K.C. Grabar, K.J. Allison, B.E. Baker, R.M. Bright, K.R. Brown, R.G. Freeman, A.P. Fox, C.D. Keating, M.D. Musick, M.J. Natan, *Langmuir* 12 (1996) 2353.
- [15] C.D. Keating, M.D. Musick, M.H. Keefe, M.J. Natan, *J. Chem. Educ.* 76 (1999) 949.
- [16] T. Murphy, H. Schmidt, H.D. Kronfeldt, *SPIE* 3107 (1997) 281.
- [17] M. Hu, S. Noda, T. Okubo, Y. Yamaguchi, H. Komiyama, *Appl. Surf. Sci.* 181 (2001) 307.
- [18] T. Murphy, H. Schmidt, H.D. Kronfeldt, *Appl. Phys. B* 69 (1999) 147.
- [19] S. Lucht, T. Murphy, H. Schmidt, H.D. Kronfeldt, *J. Raman Spectrosc.* 31 (2000) 1017.

-
- [20] H. Schmidt, N. Bich Ha, J. Pfannkuche, H. Amann, H.D. Kronfeldt, G. Kowalewska, *Mar. Poll. Bull.* 49 (2004) 229.
- [21] P. Leyton, S. Sanchez-Cortes, J.V. Garcia-Ramos, C. Domingo, M. Campos-Valette, C. Saitz, R.E. Clajivo, *J. Phys. Chem. B* 108 (2004) 17484.
- [22] P. Leyton, C. Domingo, S.Sanchez-Cortes, M. Campos-Valette, J.V. Garcia-Ramos, *Langmuir* 21 (2005) 11814.
- [23] O. Seitz, M.M. Chehimi, E. Cabet-Deliry, S. Truong, N. Felidj, C. Perruchot, S.J. Greaves, J.F. Watts, *Colloids Surf. A: Physicochem. and Eng. Aspects* 218 (2003) 225.
- [24] N. Hajdukova, M. Prochazka, J. Stepanek, M. Spirkova, *Colloids Surf. A: Physicochem. and Eng. Aspects* 301 (2007) 264.
- [25] G. Chumanov, K. Solokov, B.W. Gregory, T.M. Cotton, *J. Phys. Chem* 99 (1995) 9466.
- [26] H.Y. Jung, Y-K. Park, S. Park, S.K. Kim, *Anal. Chim. Acta* 602 (2007) 236.
- [27] H. Chen, Y. Wang, S. Dong, E. Wang, *Spectrochim. Acta Part A* 64 (2006) 343.
- [28] J.C.S. Costa, A.C. Sant'Ana, P. Corio, M.L.A. Temperini, *Talanta* 70 (2006) 1011.
- [29] B. Lee, Y. Kim, H. Lee, J. Yi, *Microporous Mesoporous Mater.* 50 (2001) 77.
- [30] Z-C. Liu, Q-G. He, P-F. Xiao, B. Liang, J-X. Tan, N-Y. He, Z-H. Lu, *Mater. Chem. Phys.* 82 (2003) 301.
- [31] Y. Fu, R. Yuan, L. Xu, Y. Chai, X. Zhong, D. Tang, *Biochem. Eng. J.* 23 (2005) 37.
- [32] U. Bexell, T.M. Grehk, *Surf. Coat. Technol.* 201 (2007) 4734.
- [33] G. Frens, *Nature, Phys. Sci.* 241 (1973) 20.
- [34] P.C. Lee, D. Meisel, *J. Phys. Chem.* 86 (1982) 3391.
- [35] O. Siiman, L.A. Bumm, R. Callaghan, C.G. Blatchord, M. Kerker, *J. Phys. Chem.* 87 (1982) 1014.
- [36] Designation D 1141-90 (reapproved 1992) from American Society for Testing Materials (ASTM).

-
- [37] R.L. Sobocinski, M.A. Bryant, J.E. Pemberton, *J. Am. Chem. Soc.* 112 (1990) 6177.
- [38] F. Osterloch, H. Hiramatsu, R. Porter, T. Guo, *Langmuir* 20 (2004) 5553.
- [39] W.R. Thompson, M. Caei, M. Ho, J.E. Pemberton, *Langmuir* 13 (1997) 2291.
- [40] J.A. Creighton, *Surf. Sci.* 124 (1983) 209.
- [41] T.G. Lee, K. Kim, M.S. Kim, *J. Phys. Chem.* 95 (1991) 9950.
- [42] S. Sanchez-Cortés, J.V. Garcia-Ramos, *J. Raman Spectrosc.* 29 (1998) 365.

Figures

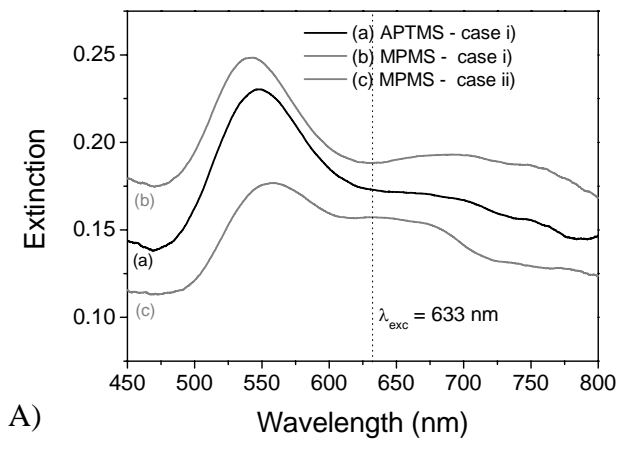
Scheme 1



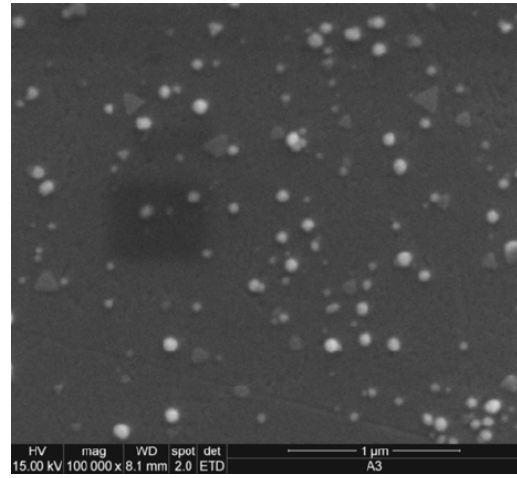
A)

B)

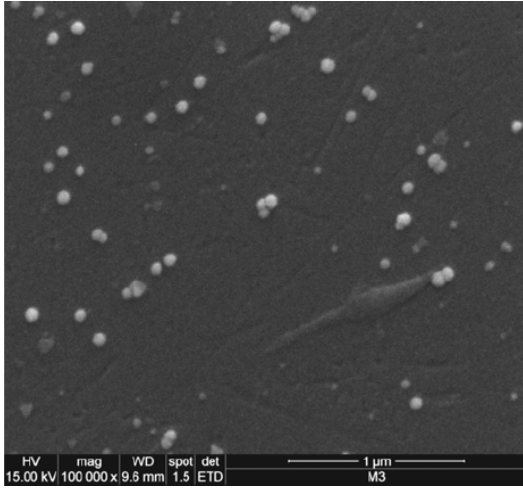
Fig1



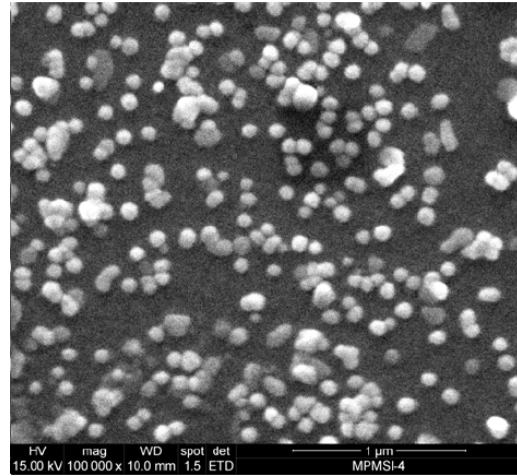
A)



B)



C)



D)

Fig2

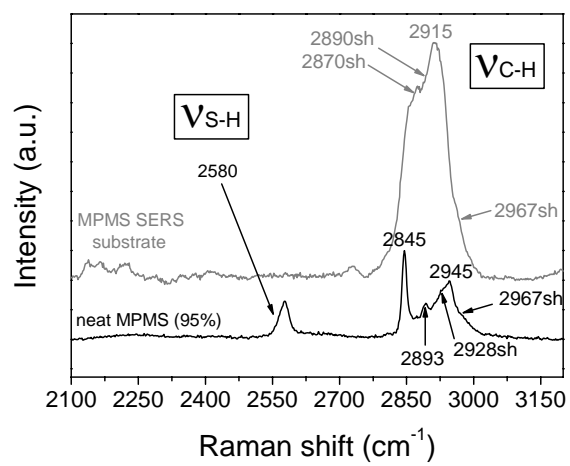


Fig3

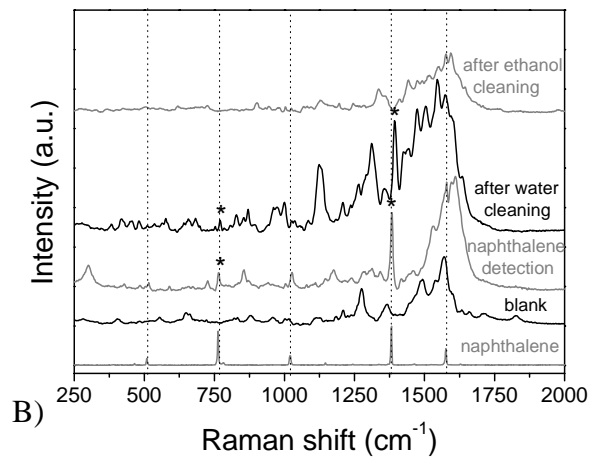
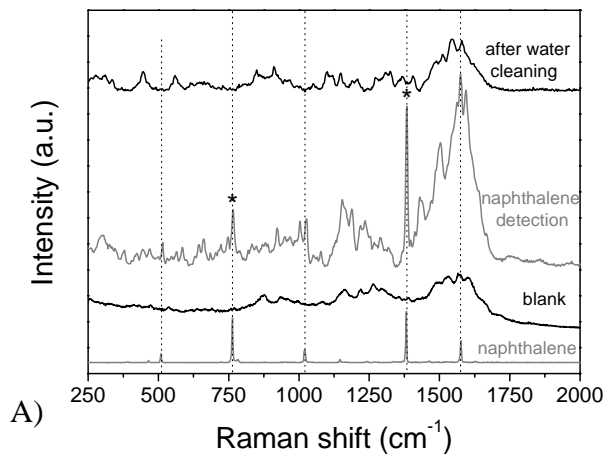


Fig4

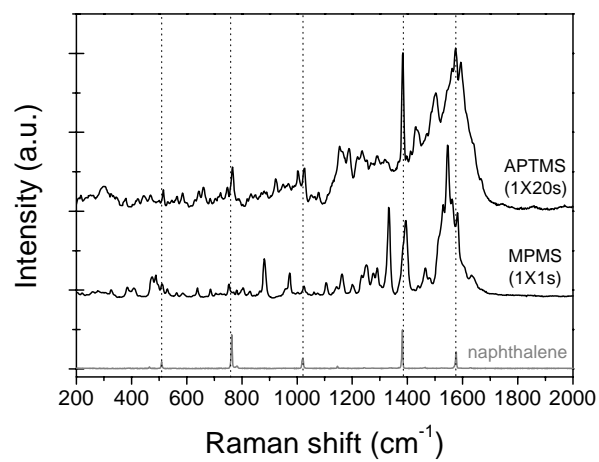
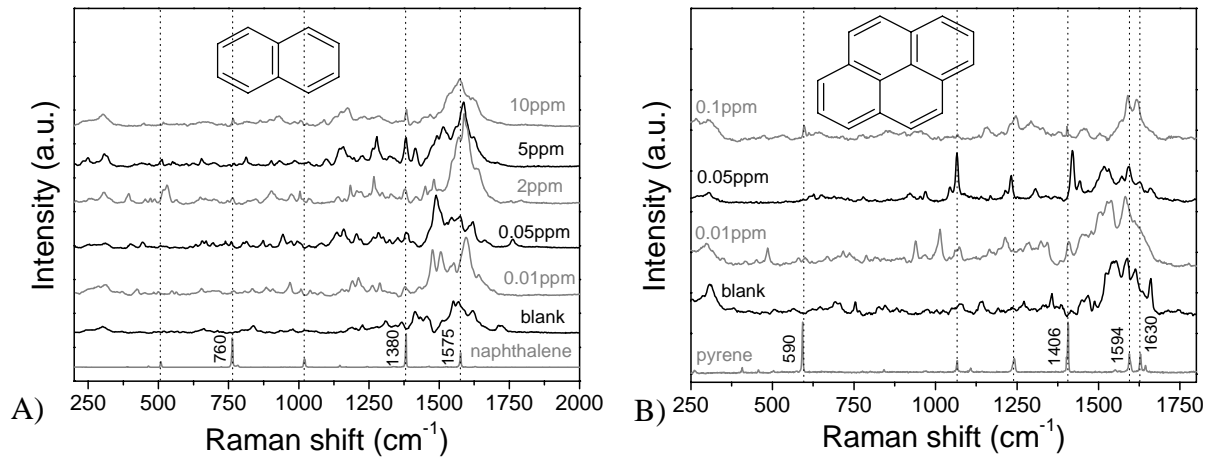


Fig5



Tables

Table 1

Raman shift (cm ⁻¹)		assignment
neat MPMS	MPMS SERS substrate	
2580	-	v(SH)
2845	sh	v _s (CH ₃)
-	2870	v _s (CH ₂)
2893	2890sh	v _a (CH ₂)
2928sh	2915	v _s (CH ₂) / v _a (CH ₂)
2945	sh	v _s (CH ₃)
2967sh	2967sh	v _a (CH ₃) / v _a (CH ₂)

sh = shoulder